



HAL
open science

Dynamical relaxation and massive extrasolar planets

John C. B. Papaloizou, Caroline Terquem

► **To cite this version:**

John C. B. Papaloizou, Caroline Terquem. Dynamical relaxation and massive extrasolar planets. Monthly Notices of the Royal Astronomical Society, 2001, 325, pp.221-230. 10.1046/j.1365-8711.2001.04386.x . hal-04110959

HAL Id: hal-04110959

<https://hal.science/hal-04110959>

Submitted on 7 Jun 2023

HAL is a multi-disciplinary open access archive for the deposit and dissemination of scientific research documents, whether they are published or not. The documents may come from teaching and research institutions in France or abroad, or from public or private research centers.

L'archive ouverte pluridisciplinaire **HAL**, est destinée au dépôt et à la diffusion de documents scientifiques de niveau recherche, publiés ou non, émanant des établissements d'enseignement et de recherche français ou étrangers, des laboratoires publics ou privés.

Dynamical relaxation and massive extrasolar planets

John C. B. Papaloizou^{1★} and Caroline Terquem^{2,3★}

¹*Astronomy Unit, Queen Mary & Westfield College, Mile End Road, London E1 4NS*

²*Institut d'Astrophysique de Paris, 98 bis Boulevard Arago, 75014 Paris, France*

³*Université Denis Diderot–Paris VII, 2 Place Jussieu, 75251 Paris Cedex 5, France*

Accepted 2001 February 8. Received 2001 February 7; in original form 2000 December 21

ABSTRACT

Following the suggestion of Black that some massive extrasolar planets may be associated with the tail of the distribution of stellar companions, we investigate a scenario in which $5 \leq N \leq 100$ planetary mass objects are assumed to form rapidly through a fragmentation process occurring in a disc or protostellar envelope on a scale of 100 au. These are assumed to have formed rapidly enough through gravitational instability or fragmentation that their orbits can undergo dynamical relaxation on a time-scale of ~ 100 orbits.

Under a wide range of initial conditions and assumptions, the relaxation process ends with either (i) one potential ‘hot Jupiter’ plus up to two ‘external’ companions, i.e. planets orbiting near the outer edge of the initial distribution; (ii) one or two ‘external’ planets or even none at all; (iii) one planet on an orbit with a semi-major axis of 10 to 100 times smaller than the outer boundary radius of the initial distribution together with an ‘external’ companion. Most of the other objects are ejected and could contribute to a population of free-floating planets. Apart from the potential ‘hot Jupiters’, all the bound objects are on orbits with high eccentricity, and also with a range of inclination with respect to the stellar equatorial plane. We found that, apart from the close orbiters, the probability of ending up with a planet orbiting at a given distance from the central star increases with the distance. This is because of the tendency of the relaxation process to lead to collisions with the central star. The scenario we envision here does not impose any upper limit on the mass of the planets. We discuss the application of these results to some of the more massive extrasolar planets.

Key words: celestial mechanics – planetary systems: formation – planetary systems: protoplanetary discs.

1 INTRODUCTION

The recent discovery of extrasolar giant planets orbiting around nearby solar-type stars (Mayor & Queloz 1995; Marcy & Butler 1998, 2000) has stimulated renewed interest in the theory of planet formation. The objects observed so far have projected masses, $M_p \sin i$, that are characteristic of giant planets, i.e. $0.4 \leq M_p \sin i \leq 11 M_J$, M_J denoting a Jupiter mass. Although $M_p \sin i$ is only a lower limit of the actual planet mass, statistical arguments suggest that in most cases mass and projected mass differ only by a factor of order unity. The orbital semi-major axes, a , are in the range $0.04 \leq a \leq 2.5$ au, and orbital eccentricities, e , in the range $0.0 \leq e \leq 0.67$ (Marcy & Butler 2000).

It is a challenge to formation theories to explain the observed masses and orbital element distributions. There are two main theories of giant planet formation (see e.g. Papaloizou & Terquem 1999 and references therein). One is the core instability scenario. In this, a solid core of several earth masses is built up in the

protostellar disc, at which point it is able to begin to accrete gas and evolve to become a giant planet. Once massive enough, it is able to open a gap in the disc and undergo orbital migration through disc–protoplanet interactions (e.g. Lin & Papaloizou 1993 and references therein). It has been suggested that the high orbital eccentricities for extrasolar planets might be explained by disc–protoplanet interactions (Artymowicz 1992).

Recent simulations of protoplanets in the observed mass range (Bryden et al. 1999; Kley 1999; Lubow, Seibert & Artymowicz 1999) interacting with a disc with parameters thought to be typical of protoplanetary discs, but constrained to be in a circular orbit, indicate gap formation and upper mass limit consistent with the observations. However, simulations by Nelson et al. (2000) that relaxed the assumption of fixed circular orbits found inward migration and that the disc–protoplanet interaction leads to strong eccentricity damping. Thus, the observed eccentricities of apparently isolated extrasolar planets are so far unexplained by this scenario.

The other possible formation mechanism is through fragmentation or gravitational instability in a protostellar disc (e.g. Cameron

★E-mail: jcbp@maths.qmw.ac.uk (JCBP); terquem@iap.fr (CT)

1978, Boss 2000). This may occur early in the life of a protostellar disc surrounding a class 0 protostar on a dynamical time-scale. Such discs have been observed (see e.g. Pudritz et al. 1996) and the characteristic size is about 100 au. It is unlikely that such a process would operate at distances smaller than about 50 au from the central star as, in the optically thick parts of the disc, non-axisymmetric density waves redistribute mass and angular momentum before fragmentation can proceed (e.g. Papaloizou & Savonije 1991; Laughlin & Bodenheimer 1994). Fragmentation is more likely when cooling is efficient, as may occur in the optically thin parts of the disc, beyond about 50 au (Papaloizou & Terquem 1999). However, the detailed conditions required for it to occur are unclear and may require constraining influences from the external environment (Pickett et al. 2000). Note that fragmentation may also occur before a disc is completely formed, during the initial collapse of the protostellar envelope. Such opacity-limited fragmentation has been estimated to produce objects with a lower mass limit of $7 M_J$ (Masunaga & Inutsuka 1999), but there is no definitive argument to rule out somewhat smaller masses (Bodenheimer, Hubickyj & Lissauer 2000). It is possible that both the disc and fragments may form simultaneously out of the envelope, the relative importance of the two processes depending for instance on the angular momentum content of the envelope, on the strength of any magnetic field (so far neglected in disc fragmentation calculations) and possibly on the initial clumpiness. Note that large-scale observations of class 0 envelopes so far do not rule out the presence of clumps with masses smaller than about $10 M_J$ (Motte & André 2001).

It is the purpose of this paper to investigate the evolution, under gravitational interactions, of a distribution of N massive planets which we assume to have been formed through a fragmentation process rapidly enough that their orbits can undergo subsequent dynamical relaxation on a time-scale of hundreds of orbits. In common with related work on orbital evolution occurring after assumed formation in a disc (e.g. Rasio & Ford 1996; Weidenschilling & Mazari 1996; Lin & Ida 1997), we shall neglect the effects of any remnant disc gas so that there are only gravitational interactions (including tidal interactions with the central star). Thus this work complements studies of the initial fragmentation process in a gaseous medium.

It turns out that the resulting evolution leads to similar end states independently of whether the initial configuration is assumed to be in the form of a spherical shell or a disc-like structure.

The motivations for this work are firstly the suggestion by Black (1997) and Stepinski & Black (2000) that massive extrasolar planets on highly eccentric orbits could actually be the low-mass tail of the low-mass companion distribution to solar-like stars produced by fragmentation processes. Here, we wish to investigate to what extent that planets with orbital elements similar to those observed can be produced, and in particular whether or not ‘hot Jupiters’ orbiting close to the star can be formed. Secondly, we consider the recently detected population of free-floating planets and its relationship to that of planets orbiting solar-type stars (Lucas & Roche 2000, Zapatero Osorio et al. 2000). It is of interest to know to what extent free-floating planets could be produced as a result of ejection from the neighbourhood of a star.

We have considered the orbital evolution of N bodies with masses in the giant planet range, which are assumed to be formed rapidly, using up the gas in a protostellar disc or envelope around a solar mass star, so that they can undergo subsequent dynamical relaxation on a time-scale of ~ 100 orbits. We have performed calculations with $5 \leq N \leq 100$.

In all the runs we performed, most of the planets were ejected from the system and at most three planets remained bound to the central star. We found that close encounters with the central star occurred for about 10 per cent of the planets for all values of N considered. Such close encounters early in the evolution tended to result in collisions. These tended to be avoided at later times, so that tidal interaction might then result in orbital circularization at fixed pericentre distance, leading to the formation of a very closely orbiting giant planet.

Typically the runs ended up with either (i) one potential ‘hot Jupiter’ plus up to two ‘external’ companions, i.e. planets orbiting near the outer edge of the initial distribution; (ii) one or two ‘external’ planets or even none at all; (iii) one planet on an orbit with a semi-major axis of 10 to 100 times smaller than the outer boundary radius of the initial distribution, together with an ‘external’ companion. Apart from the potential ‘hot Jupiters’, all these objects are on orbits with high eccentricity, and also with a range of inclination with respect to the stellar equatorial plane. We found that, apart from the close orbiters, the probability of ending up with a planet orbiting at a given distance from the central star increases with the distance.

The objects that become unbound may contribute to a population of freely floating planets (Lucas & Roche 2000; Zapatero Osorio et al. 2000) which could be several times larger than that of giant planets found close to the central star.

Thus the dynamical relaxation process considered here may operate in some cases to produce giant planets with high orbital eccentricity at several astronomical units from their central star as well as closely orbiting planets. In all cases a population of loosely bound planets is also expected.

The plan of this paper is as follows. In Section 2 we describe the model and basic equations used. In Section 3 the initial conditions are formulated and in Section 4 the physics of the relaxation process is discussed. In Section 5 we present our numerical results and in Section 6 we summarize and discuss them.

2 THE MODEL AND BASIC EQUATIONS

We consider a system consisting of N planets and a primary star moving under their gravitational attraction. As we are interested in possible close approaches to, or collisions with, the central star, we adopt a spherical polar coordinate system (r, θ, φ) with the origin at the stellar centre. The planets and central star are treated as point masses. However, to take into account the possible losses of orbital energy and angular momentum to the stellar material, a simple model for taking into account the tidal interaction between the star and a closely approaching planet is also included.

The equations of motion are:

$$\frac{d^2 \mathbf{r}_i}{dt^2} = -\frac{GM_* \mathbf{r}_i}{|\mathbf{r}_i|^3} - \sum_{j=1}^N \frac{GM_j \mathbf{r}_{ij}}{|\mathbf{r}_{ij}|^3} - \mathbf{a} + \mathbf{F}_{Ti}. \quad (1)$$

Here M_* , M_i , \mathbf{r}_i and \mathbf{r}_{ij} denote the mass of the central star, the mass of planet i , the position vector of planet i , and $\mathbf{r}_i - \mathbf{r}_j$, respectively. The acceleration of the coordinate system based on the central star (indirect term) is:

$$\mathbf{a} = \sum_{j=1}^N \frac{GM_j \mathbf{r}_j}{|\mathbf{r}_j|^3} \quad (2)$$

and that caused by tidal interaction with planet i is \mathbf{F}_{Ti} .

In the situation envisaged here, tidal interactions occur when a

planet has a close encounter with the star. When this occurs, the planet approaches from large distances on an almost parabolic orbit. The time between successive encounters will then be long compared to that for the tidal interaction itself. Accordingly, we approximate the process as a sequence of independent energy and angular momentum transfers that occur at each periastron passage. We utilize the results of Press & Teukolsky (1977) who calculated these transfers in the small perturbation limit for a non-rotating star modelled as a polytrope and a perturber on a parabolic orbit. We shall neglect the effects of tides acting on the planet itself. Accordingly, our model is simplified. However, it does enable us to include tidal effects and demonstrate how they start to lead to orbital circularization and gravitational decoupling of an inner planet from the others as it moves on to a close orbit. However, it is only applicable while the planet orbit has high eccentricity.

We adopt a form for F_{Ti} that is able to give approximately the correct angular momentum and energy exchanges with the star on a close approach but which is negligible at larger distances from the central star:

$$F_{Ti} = -\frac{GM_i R_*^5 R_{pi}^3 T_1}{C_1 |j_i| |r_i|^{11}} (|r_i|^2 \mathbf{v}_i - \mathbf{v}_i \cdot \mathbf{r}_i \mathbf{r}_i). \quad (3)$$

Here j_i is the specific angular momentum of planet i , \mathbf{v}_i is its velocity vector, R_* is the stellar radius, $R_{pi} = j_i^2 / (2GM_*)$ is the distance of closest approach of planet i assuming a parabolic orbit, $C_1 = 2\sqrt{\pi}/3$ and $T_1 = 0.6/[1 + (R_{pi}/R_*)^3]$.

The equations of motion are here integrated using the Bulirsch–Stoer method (e.g. Press et al. 1993).

Using equation (3), we can derive the energy lost to the star during a close encounter of planet i , assumed on a parabolic orbit, as

$$\Delta E = -\int_{-\infty}^{\infty} M_i F_{Ti} \cdot \mathbf{v}_i dt \quad (4)$$

where, because of the rapid convergence of the integral, the limits are extended to $\pm\infty$. This gives

$$\Delta E = \frac{GM_i^2 R_*^5 T_1}{R_{pi}^6}, \quad (5)$$

which gives values coinciding approximately with values given by Press & Teukolsky (1977).

We comment that, according to equation (5), a star grazing encounter on a parabolic orbit results in a final semi-major axis $a \sim 1.7R_* M_*/M_i$. For a central solar mass with $R_* = 10^{11}$ cm and $M_i \sim 1 M_J$, $a \sim 10$ au. Thus, bound orbits with $a \sim 10$ au are significantly modified if they have a close encounter with the central star. Note too that the energy exchange rates are small for the planetary mass objects considered here, giving some justification for the linear approximation used to calculate them.

3 INITIAL CONDITIONS

The simulations performed here were begun by placing N planets in some specified volume in a random location chosen to give a Monte Carlo realization of a prescribed density distribution. We considered both the case of a uniform density spherical shell with $R_{\min} \leq r \leq R_{\max}$ and that of a thick annulus with $R_{\min} \leq r \leq R_{\max}$ occupying $\cos^{-1}(0.1) \leq \theta \leq \cos^{-1}(-0.1)$ with a density $\propto r^{-2}$, where r is the spherical radius and θ the co-latitude. For the calculations presented here, $R_{\min} = 0.1R_{\max}$ and $0.5R_{\max}$ for the

annulus and the spherical shell, respectively. The planets were then given the local circular velocity in the azimuthal direction. Note that because of the spatial placements the initial orbits are not coplanar. In some cases the planets were taken to have equal mass M_p , while in others each planet was allocated a mass qM_p where q was a random number between zero and one. In the latter case the mass distribution of the protoplanets does not correspond to the specified density distribution, indicating some redistribution of mass among the embryos.

In general the various initial conditions we have considered lead to the same qualitative evolution.

However, it must be emphasized that the systems are chaotic with the consequence that very small detailed changes to the initial conditions or the integration procedure will in general lead to very different results in detail. To deal with this issue one can adopt the notion of shadow orbits (Quinlan & Tremaine 1992). According to this, one can expect that although inevitable small errors lead to a significant deviation of the numerical solution from the actual one, there is another solution of the real system obtained with slightly different initial conditions which remains close to the numerical one. Thus, we should be able to identify qualitative trends in the evolution of an ensemble of systems of the type we consider and we restrict ourselves to that.

3.1 Scale invariance

We comment that the equations we solve, incorporating tidal effects, have a radial scale invariance. Thus, all radii may be multiplied by some factor f while the time-scales are multiplied by $f^{3/2}$. The size of the central star has to be scaled by the factor f also. Here we shall take the unit of length to be R_{\max} . Then the stellar radius is specified through R_*/R_{\max} . The time unit is the period of a circular orbit at R_{\max} , $P_0 = 2\pi R_{\max}^{3/2} / \sqrt{GM_*}$. The interactions amongst the planets lead to some escaping the system. Objects with positive energy which had reached a distance βR_{\max} were considered to be escapers. We have considered $\beta = 20$ and $\beta = 100$ which both lead to the same qualitative picture.

4 EVOLUTION RELAXATION AND STAR GRAZERS

Even the systems which have a small number of bodies are found to interact strongly and to undergo relaxation like a stellar system (Binney & Tremaine 1987). For such a system, the relaxation time is:

$$t_R = \frac{0.34v^3}{3\sqrt{3}G^2 M_p \rho \ln(\Lambda)}. \quad (6)$$

Here the root mean square velocity is v , ρ is the mass density of interacting bodies assumed, for simplicity, to have equal mass M_p , and $\Lambda = M_*/M_p$.

Using $v^2 = GM_*/r$, $NM_p = 4\pi r^3 \rho/3$ and adopting the orbital period $P = 2\pi r/v$ this becomes

$$t_R = \frac{0.044M_*^2 P}{M_p^2 N \ln(M_*/M_p)}. \quad (7)$$

Thus, for $M_p/M_* = 5.0 \times 10^{-3}$ and $N = 5$, the relaxation time is about 100 orbits. For systems with r in the 100 to 1000-au range, this time is around 10^5 – 10^6 y, which is within the estimated lifetimes of protostellar discs.

The evolution we obtain is similar to that undergone by spherical

star clusters (Binney & Tremaine 1987). The relaxation, caused by binary encounters, causes some objects to attain escape velocity while others become more bound. Eventually, all either escape or end up in extended orbits, except for one body which takes up all the binding energy. This is a generic result, provided that close encounters with the star can be avoided. However, for the parameters range of interest such encounters are likely. The situation resembles that of the accretion of stars from a spherical star cluster by a black hole (e.g. Frank & Rees 1976). At a location with radius r , the fractional volume of phase space containing orbits that would collide with the star if unperturbed is $\sim R_*/r$ (this being the ratio of the square of the angular momentum below which an impact is expected to the square of the mean angular

momentum). If an object cannot diffuse out of this volume before impact, the mean time before diffusion into the effective volume produces an impact, for a particular object, is $\sim t_R$. However, the time to diffuse out of the effective volume is $\sim (R_* t_R)/r$. If this time is less than the crossing time $t_c \sim r/v$, the expected mean time to impact is $t_{\text{enc}} = (r t_c)/R_*$. This time is just the crossing time divided by the probability of being in the effective volume of phase space which is regularly sampled because of the effective diffusion (see Frank & Rees 1976).

In our calculations, the innermost most tightly bound object undergoes relaxation or phase space diffusion which can lead to close encounters. For $r = 25$ au, $t_c \sim 20$ y, and $R_* \sim 1.5 \times 10^{11}$ cm, $t_{\text{enc}} \sim 5 \times 10^4$ y. Thus we can expect close encounters to occur within the general relaxation process. In some cases these can lead to a strong tidal interaction, which can circularize the orbit and potentially lead to the formation of a ‘hot Jupiter’.

Table 1. This table lists the parameters for each simulation: the number of planets N , the ratio of stellar radius to R_{max} and the initial set up In , where $n = 1, 2$ denotes spherical shell and thick annulus, respectively. The last column contains M_p/M_* , with (R) denoting that the masses were allocated uniformly at random in the interval $(0; M_p)$.

| Run | N | R_*/R_{max} | In | M_p/M_* |
|-----|-----|------------------------|------|------------------------|
| 1 | 5 | 0.0 | I2 | 5×10^{-3} |
| 2 | 10 | 9.396×10^{-5} | I1 | 5×10^{-3} |
| 3 | 10 | 1.337×10^{-4} | I2 | 5×10^{-3} |
| 4 | 8 | 1.337×10^{-4} | I2 | 5×10^{-3} (R) |
| 5 | 40 | 9.396×10^{-5} | I1 | 5×10^{-3} |
| 6 | 100 | 9.396×10^{-5} | I1 | 1×10^{-2} (R) |

5 NUMERICAL RESULTS

Here we describe a sample of our results that illustrate the characteristic behaviour exhibited by the systems we consider. The calculations presented are listed in Table 1. We note that if $R_{\text{max}} = 100$ au, then $R_*/R_{\text{max}} = 9.396 \times 10^{-5}$ or 1.337×10^{-4} correspond to $R_* = 2$ or $3 R_\odot$, respectively, which is the radius of a protostar with a mass of roughly $1 M_\odot$ in the early stages.

Run 1 corresponds to a system of $N = 5$ planets each having a mass $5 \times 10^{-3} M_*$. Fig. 1 shows plots of a/R_{max} in a logarithmic scale, where a denotes the semi-major axis for each planet in the

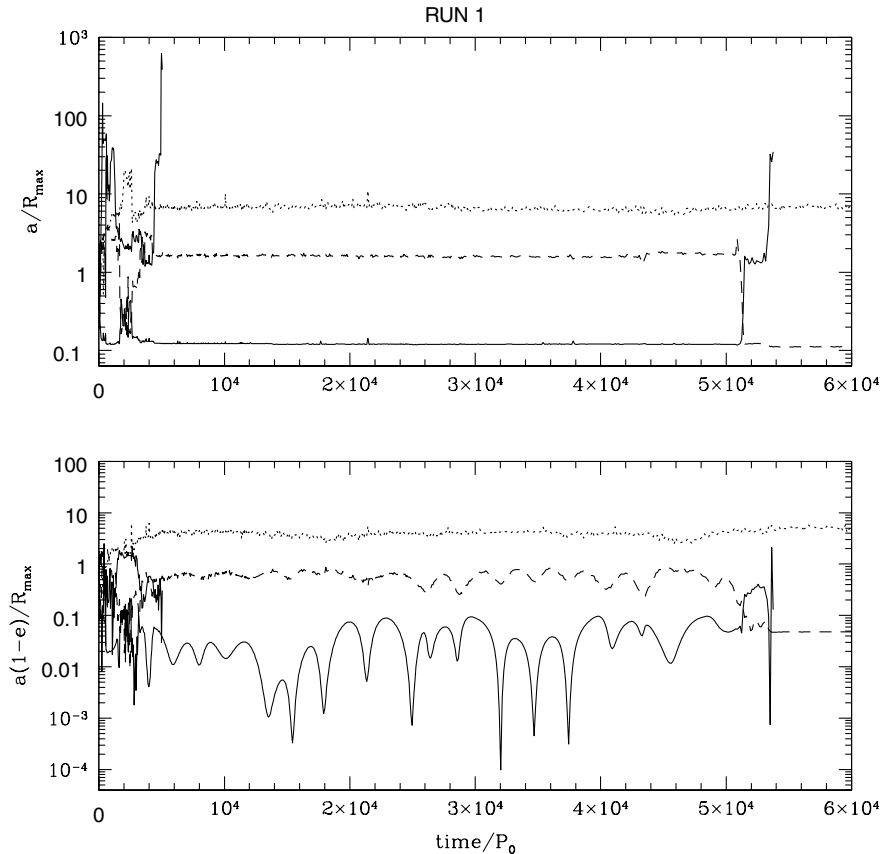


Figure 1. This figure shows the evolution of the semi-major axes (*upper plot*) and pericentre distances (*lower plot*) of the five planets in the system versus time (measured in units of P_0) for run 1 in Table 1. The lines correspond to the different planets, each having a mass $5 \times 10^{-3} M_*$. In this and other similar figures, a line terminates just prior to the escape of a planet. In this case $R_* = 0$ so that there was no tidal interaction with the central star. Note that the time resolution in this and similar figures is not fine enough for all close approaches to the star to be fully represented.

system, versus time (measured in units of P_0). Each line corresponds to a different planet. During the run, three planets escape, shown in the figure by lines that terminate just prior to escape. For this case $R_* = 0$ so that there was no tidal interaction with the central star. The initial relaxation time for this and other similar cases is on the order of $100P_0$, in agreement with equation (7). The evolution of $a(1-e)/R_{\max}$, $a(1-e)$ being the pericentre distance and e being the eccentricity, is also shown in Fig. 1. We see that approaches to within $\sim 10^{-2}R_{\max}$ of the central star occur for the innermost object on a time-scale of the same order of magnitude as the relaxation time. This is a common feature of the simulations presented here. Note that for $R_{\max} = 100$ au, the closest approach is to within $\sim 3 \times 10^{11}$ cm, which is comparable to a solar radius. After about $6000P_0$, the main relaxation is over with nearly all the binding energy being contained within one object with $a \sim 0.1R_{\max}$ and $e \sim 0.9$. However, after about $5 \times 10^4 P_0$, the two innermost planets have a close approach which results in their position being exchanged and one of them being ejected. The end result of this run is then two planets on well-separated orbits. The innermost planet has $a \sim 0.1R_{\max}$ and $e \sim 0.5$.

A plot of the evolution of the semi-major axes and pericentre distances versus time (measured in units of P_0) for Run 2 in Table 1 is given in Fig. 2. For this run, the initial number of planets is $N = 10$, and $R_*/R_{\max} = 9.396 \times 10^{-5}$, so that tidal effects operate. After about $10^4 P_0$, there are only two planets still bound to the star. The others have been ejected. The innermost planet which is left has $e = 0.66$ and $a \sim 0.02R_{\max}$. If $R_{\max} = 100$ au, this corresponds to $a \sim 2$ au.

Fig. 3 shows the evolution of the semi-major axes and pericentre

distances versus time (measured in units of P_0) for Run 3 in Table 1. For this run $N = 10$ and $R_*/R_{\max} = 1.337 \times 10^{-4}$. The plot terminates at about $3.4 \times 10^4 P_0$, just before the innermost planet has a close encounter with the star. The evolution toward the end of the run is zoomed on in Fig. 4. We see that the semi-major axis decreases significantly, down to about $10^{-2}R_{\max}$, whereas the pericentre distance varies much less. This indicates a tidal interaction with the star. The run, if continued much further, becomes inaccurate because of our crude treatment of tides, as mentioned in Section 2. At that point we expect the orbit to circularize at a fixed pericentre distance. Evolution of this type, which is also quite common in our simulations, could potentially lead to a ‘hot Jovian-mass planet’.

Fig. 5 shows the evolution of the semi-major axes and pericentre distances versus time (measured in units of P_0) for Run 4 in Table 1. In this case $N = 8$, $R_*/R_{\max} = 1.337 \times 10^{-4}$ and the masses were selected uniformly at random in the interval $(0; 5 \times 10^{-3} M_*)$. Here again, after about $3 \times 10^4 P_0$ there are only two planets still bound to the star. The innermost planet has $e = 0.25$ and $a \sim 0.04R_{\max}$, which would correspond to 4 au in a 100-au annulus.

We now consider runs with larger N . Fig. 6 shows the evolution of semi-major axes and pericentre distances versus time (measured in units of P_0) for Run 5 in Table 1. In this case $N = 40$ and $R_*/R_{\max} = 9.396 \times 10^{-5}$, and again there are only two planets bound to the star, this time after about $8000P_0$. The others have either been ejected or have collided with the central star. Our treatment of tides is too crude to be certain about the orbital evolution of planets on very eccentric orbits which have grazing approaches to the star. In our simulations, such approaches result in

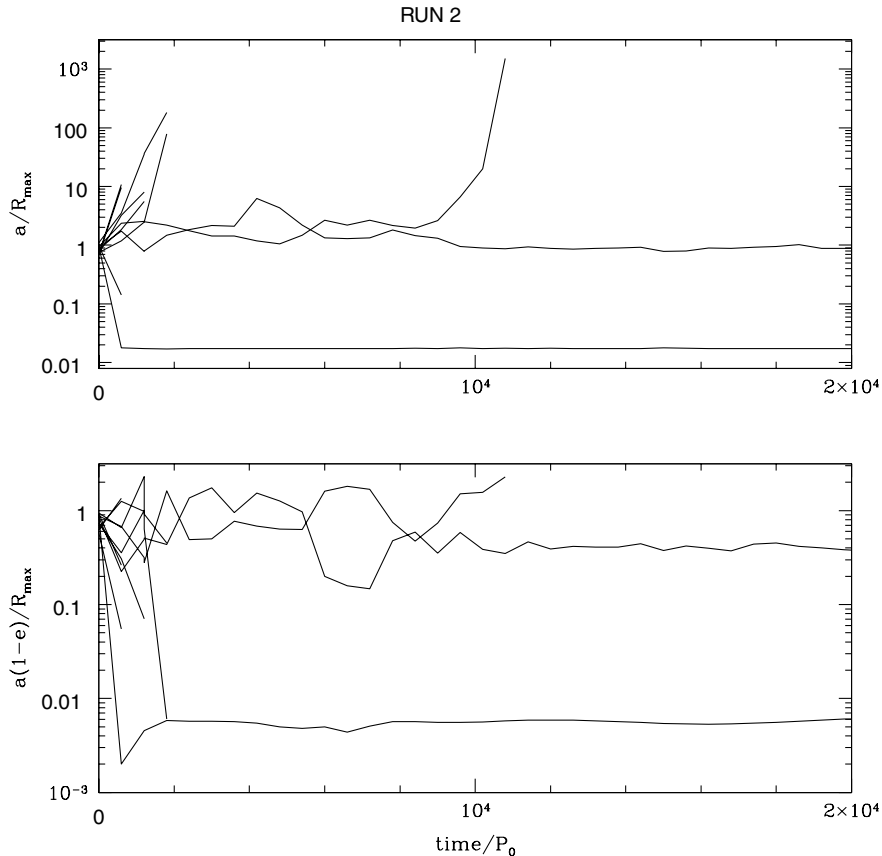


Figure 2. Same as Fig. 1 but for Run 2 in Table 1. For this run $N = 10$ and $R_*/R_{\max} = 9.396 \times 10^{-5}$.

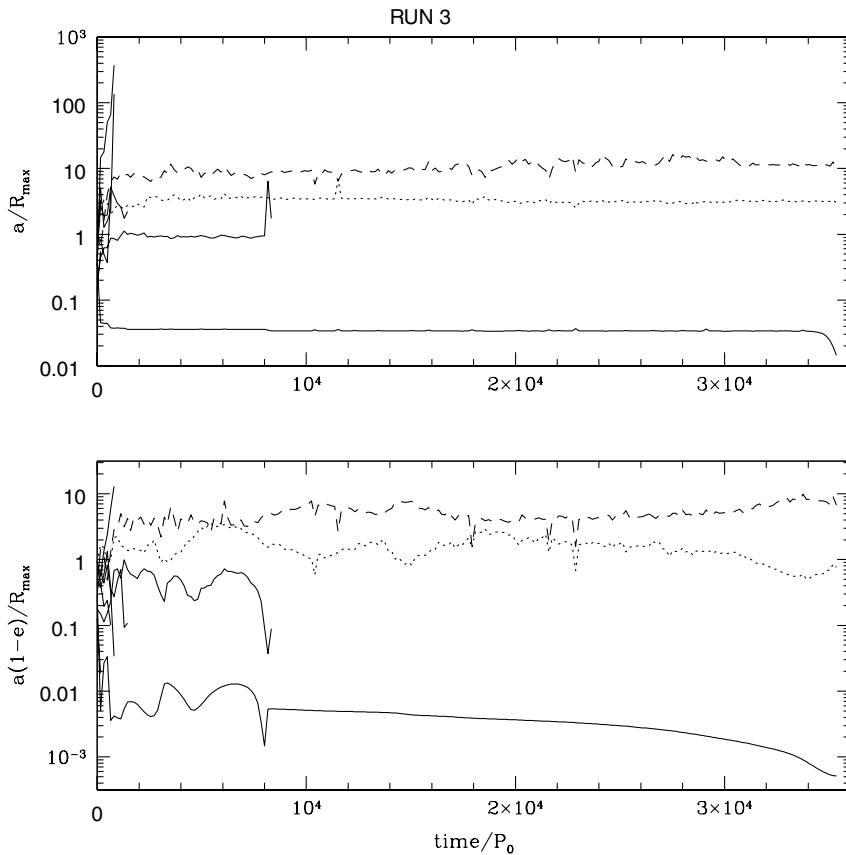


Figure 3. Same as Fig. 1 but for Run 3 in Table 1. For this run $N = 10$ and $R_*/R_{\max} = 1.337 \times 10^{-4}$. The plot terminates just before the innermost planet has a close encounter with the star.

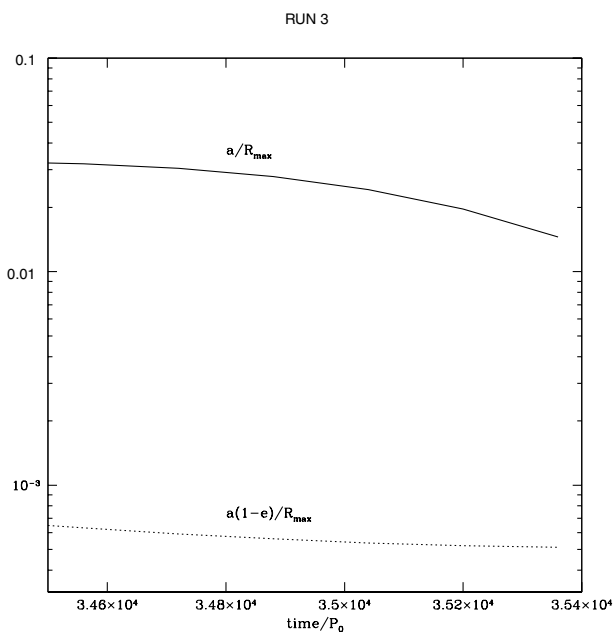


Figure 4. This figure shows the evolution of the semi-major axis (*solid line*) and the pericentre distance (*dotted line*) of the innermost planet in Run 3 versus time (measured in units of P_0) for a short interval after this planet enters a tidal interaction phase. This is a zoom on the curves displayed in Fig. 3.

the planet being lost. As far as the subsequent evolution of the system is concerned however, it does not matter whether the planet indeed hits the star or gets circularized on a close orbit. In this run, evolution occurs on a shorter time-scale as a result of the larger number of planets. Here the innermost planet has $e \sim 0.9$ and $a \sim 0.03R_{\max}$, which is 3 au if $R_{\max} = 100$ au.

Fig. 7 shows the evolution of the semi-major axes versus time (measured in units of P_0) for the only two planets in the system which have not either been ejected or collided with the central star after about $180 P_0$, for Run 6 in Table 1. Also shown are the pericentre distance and the apocentre distance for these planets. Here $N = 100$, $R_*/R_{\max} = 9.396 \times 10^{-5}$ and the masses were selected uniformly at random in the interval $(0-10^{-2} M_*)$. We see from Fig. 7 that at a time of about $1.5 \times 10^4 P_0$ the apocentre and the pericentre of the innermost and outermost planets, respectively, are very close to each other. The innermost planet then suffers a gravitational scattering by the more massive outermost planet, which results in an increase of its eccentricity and eventually a collision with the central star. We are then left with one planet with $e = 0.85$ and $a \sim 0.7R_{\max}$.

6 SUMMARY AND DISCUSSION

We have considered the orbital evolution of N bodies with masses in the giant planet range, which are assumed to have formed rapidly enough that they can undergo subsequent dynamical relaxation on a time-scale of ~ 100 orbits.

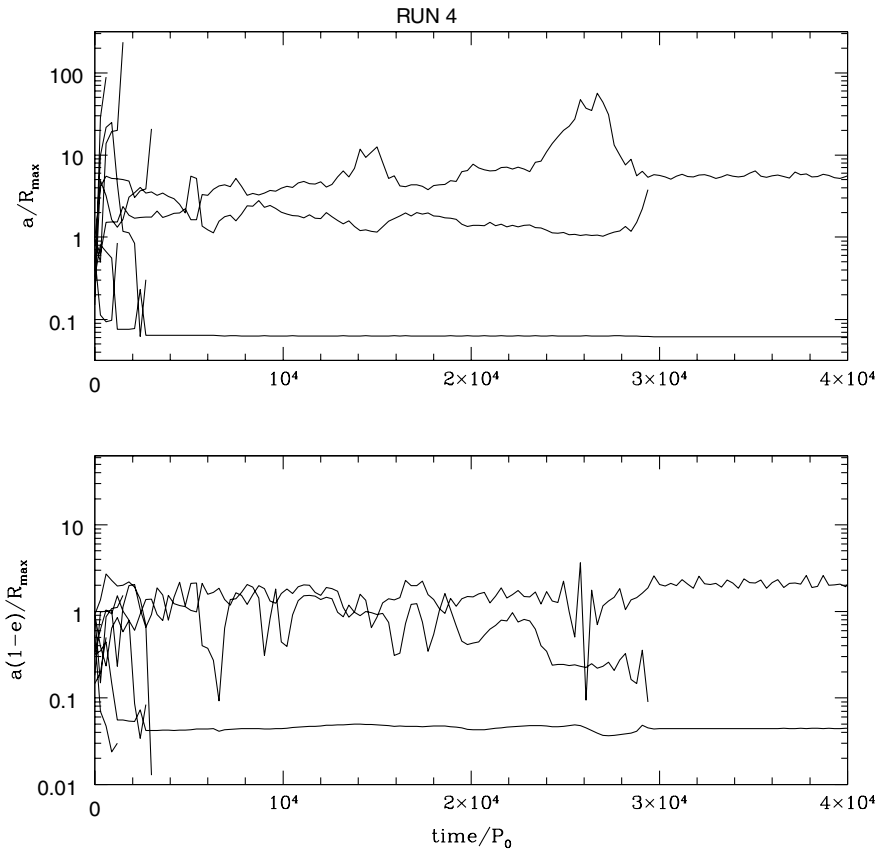


Figure 5. Same as Fig. 1 but for Run 4 in Table 1. For this run $N = 8$, $R_*/R_{\max} = 1.337 \times 10^{-4}$ and the masses were selected uniformly at random in the interval $(0; 5 \times 10^{-3} M_*)$. At the end of the run only two planets remain bound to the central star.

We have considered $5 \leq N \leq 100$. We assume that rapid formation may occur as a result of fragmentation triggered by gravitational instabilities or clumping, either in a spherical envelope during the initial protostellar collapse phase or in a disc-like configuration (e.g. Pudritz et al. 1996) as it forms. But note that because magnetic fields may play a role, the disc may not be entirely centrifugally supported. We have considered initial distributions of planets with masses in the range of 5 to $10 M_J$ that are in the form of a spherical shell or are disc-like. However, final outcomes are independent of this. In our calculations, along with previous work related to the core accretion model (Rasio & Ford 1996; Weidenschilling & Mazari 1996; Lin & Ida 1997), we neglect the effects of gas, thus the efficiency of fragmentation is assumed to be maximal.

Although our results can be applied to different radial scales, we focus the discussion below on distributions with an outer radius of 100 au, this being the dimension of observed protostellar discs in class 0 objects (e.g. Pudritz et al. 1996).

This work has been partly motivated by the suggestion by Black (1997) and Stepinski & Black (2000) that some massive extrasolar planets could actually belong to the low-mass tail of the distribution of low-mass companions to solar-like stars. That suggestion is derived from the observation that extrasolar planets that are far enough from the star that tidal circularization does not operate tend to have highly eccentric orbits.

Altogether, we have run about 25 cases with $30 \leq N \leq 100$ and many more with $N \leq 10$. We have described six representative runs in detail in this paper. Independently of how many planets we began with, the initial set-up and the technical details of the

computation, we obtained the same sets of characteristic behaviour and end states. In every case, most of the planets were ejected from the system and at most three planets remained bound to the central star after a time typically of the order of a few 10^4 outer periods P_0 . The dynamical relaxation phase is shorter when the initial number of planets is larger, but when the number of planets is reduced to less than 10 the system evolves in the same way as the systems that had a smaller initial number of planets.

We found that close encounters with the central star often occurred (for about 10 per cent of the planets) for all the values of N considered. At an early stage these tended to result in direct collisions. When a direct collision is avoided, tidal interaction between the star and a planet on a very eccentric orbit may result in orbital circularization at fixed pericentre distance, which might ultimately lead to the formation of a very closely orbiting giant planet.

As far as we could monitor the runs presented here, we did not find any physical collisions between the planets themselves. This is consistent with Lin & Ida (1997), who found that such collisions were very rare when, as in this paper, mutual tidal interactions between the planets were assumed to be ineffective. If physical collisions were to occur, they would not be expected to affect the typical outcome of our runs.

Typically, the runs ended up with either (i) one potential ‘hot Jupiter’ plus up to two ‘external’ companions, i.e. planets orbiting near the edge of the initial distribution; (ii) one or two ‘external’ planets or even none at all because a gravitational scattering between two planets may result in one being ejected and the other one colliding with the star; (iii) one planet on an orbit with a

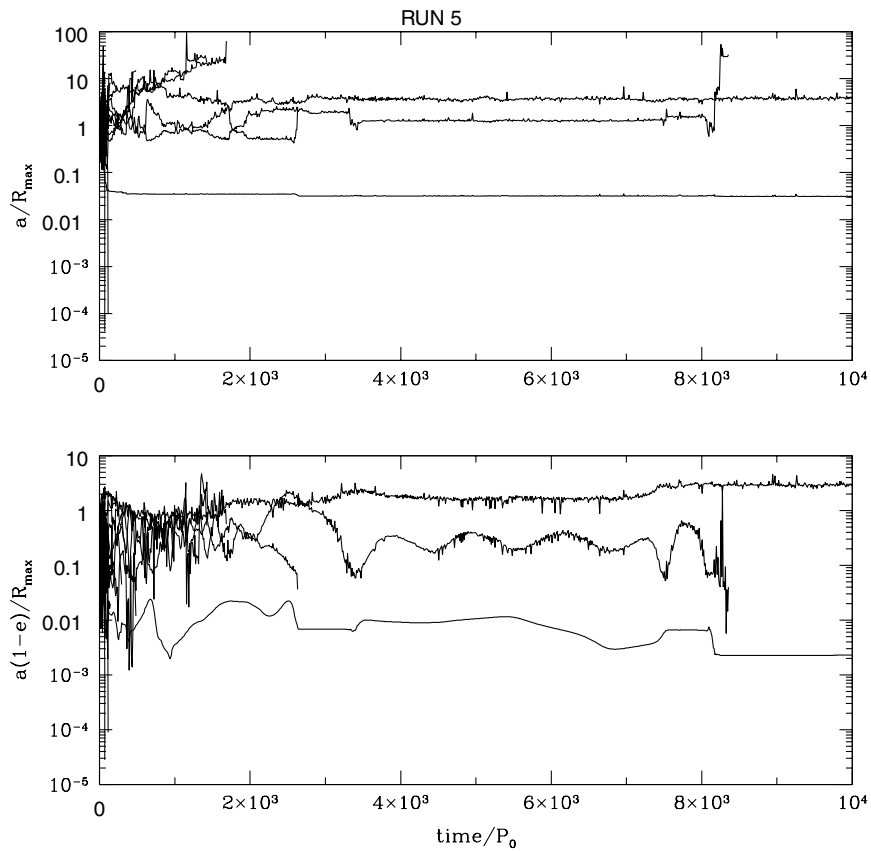


Figure 6. Same as Fig. 1 but for Run 5 in Table 1. For this run $N = 40$ and $R_{\text{sc}}/R_{\text{max}} = 9.396 \times 10^{-5}$. At the end of the run only two planets remain bound to the central star.

semi-major axis of 10 to a 100 times smaller than the initial distribution, e.g. $a \sim 1\text{--}10$ au for a 100-au distribution, plus one ‘external’ companion. Apart from the potential ‘hot Jupiters’, all these objects are on orbits with high eccentricity, and also with a range of inclination with respect to the stellar equatorial plane.

We found that, apart from the ‘hot Jupiters’, the probability of ending up with a planet orbiting at a given distance from the central star increases with the distance. Thus, this scenario produces a decreasing number of planets as we go from 100 au down to 0.1 au. This is expected, because a planet on a highly eccentric orbit has more chance of colliding with the central star as it gets closer to it. Paradoxically, the action of the central star tends to clear out a large cavity around it.

We now turn to the characteristics of some of the extrasolar planets detected so far. We restrict our attention to those with a projected mass $M_p \sin i > 4.5 M_J$, consistent with the larger masses expected for formation through fragmentation. There are seven such objects, around HD 190228, UA3, HD 2222582, HD 10697, 70 Vir, HD 89744 and HD 114762. All have an eccentricity larger than 0.12, and for six of them $e \geq 0.33$. The semi-major axis is in the range 0.88–2.5 for five of the objects, while the others have $a = 0.3$ and 0.43, respectively. The characteristics of these planets might be accounted for by our scenario, though the two cases with small a would only occur with a small probability.

Amongst the ‘hot Jupiters’ detected so far, τ Boo is particularly massive with $M_p \sin i \sim 4 M_J$. This planet is clearly a candidate for being produced by a mechanism of the type that we consider. If other ‘hot Jupiters’ began with a high mass which subsequently decreased significantly as a result of Roche

lobe overflow (Trilling et al. 1998), they could also be candidates for our model.

The scenario we envision here does not impose any upper limit on the mass of the planets, in contrast to the core accretion model, where gap formation in the gaseous nebula eventually isolates the planet from the reservoir of gas (Papaloizou & Lin 1993). Therefore, it may be relevant to the unusual planetary system recently detected around HD 168443, which has two planets with $M_p \sin i = 7.7 M_J$, $a = 0.29$ au and $e = 0.53$, and $M_p \sin i = 17.2 M_J$, $a = 2.9$ au and $e = 0.20$ respectively (Marcy et al. 2001). The high mass of the outermost planet makes it potentially a product of the mechanism considered in this paper.

The process of dynamical relaxation we have discussed here leads to planetary orbits which have a range of inclination with respect to the stellar equatorial plane. Observations of transits would therefore be a useful constraint if they could provide a measure of this inclination. Note however that, for the one transit observed so far, only an upper limit of 30° is derived for the angle between the orbital plane and the stellar equatorial plane (Queloz et al. 2000).

The objects expelled as a result of the type of relaxation process we consider may produce a population of freely floating planets (Lucas & Roche 2000; Zapatero Osorio et al. 2000) which is several times larger than that of giant planets close to the central star. This population would be expected to be typically at least 10 times larger than the population of massive planets orbiting around the star, and depends on the initial number of planets in the distribution. However, note that the population of planets orbiting central stars that went through a relaxation process of the type we

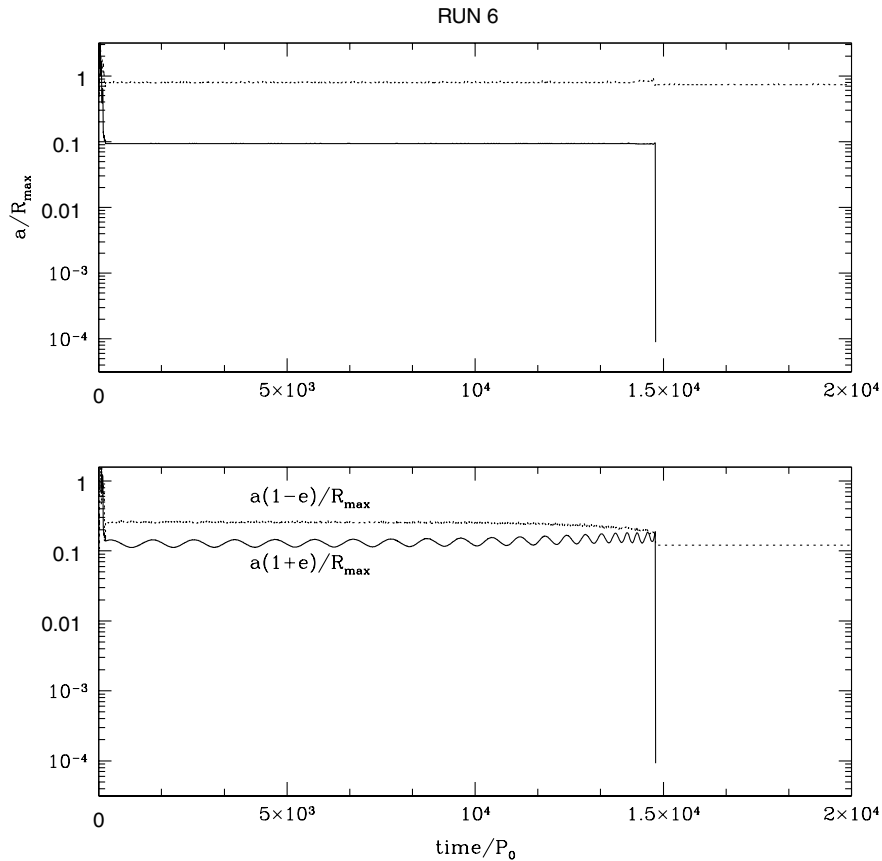


Figure 7. The *upper plot* shows the evolution of the semi-major axes of the only two planets in the system which have not either been ejected or collided with the central star after about $180 P_0$ versus time (measured in units of P_0) for Run 6 in Table 1. The *lower plot* shows the pericentre distance (*dotted line*) and the apocentre distance (*solid line*) for these planets. Here $N = 100$, $R_{\text{in}}/R_{\text{max}} = 9.396 \times 10^{-5}$ and the masses were selected uniformly at random in the interval $(0; 10^{-2} M_{\odot})$. The innermost planet suffers a gravitational scattering by the more massive outermost planet when their orbits cross which results in an increase of its eccentricity and eventually a collision with the central star.

consider may be significantly smaller than the total if planets are also independently formed through a core accretion process.

The model we have considered in this paper has of course some limitations. In particular, we have not included the effect of gas which is probably still significant in the early stages of the evolution of these systems, and which may result in more planets orbiting at smaller distances from the central star. Neither have we considered the effects of Roche lobe overflow for the planets which have a close encounter with the central star (Trilling et al. 1998) which may significantly reduce their mass.

The considerations above lead to the suggestion that there may be two populations amongst the extrasolar planets detected so far. Some of the more massive objects may be produced through fragmentation of an envelope or a disc-like structure followed by dynamical relaxation. Other predominantly lower mass objects could be produced in a disc as a result of the ‘core accretion’ model. We would of course expect to also have hybrid systems, in which both processes have occurred. The relative importance of these processes may depend for instance on the physical parameters, such as the angular momentum content, of the parent cloud.

If the scenario presented here is indeed effective in planet formation, we would expect additional massive planets to be detected further from the central star, and an important distribution of loosely bound, or ‘free-floating’ objects associated with these systems.

ACKNOWLEDGMENTS

We thank David Black for useful comments on an earlier draft of this paper. JCBP acknowledges visitor support from the University Paris VI and the IAP where part of this work was carried out. The authors thank the participants of the EARA workshop ‘Discs, Extrasolar Planets and Brown Dwarfs’ held at the IAP in July 2000 for useful discussions.

REFERENCES

- Artymowicz P., 1992, *PASP*, 104, 769
- Binney J. J., Tremaine S. D., 1987, *Galactic Dynamics*. Princeton Univ. Press, Princeton, NJ
- Black D. C., 1997, *ApJ*, 490, 171
- Bodenheimer P., Hubickyj O., Lissauer J. J., 2000, *Icarus*, 143, 2
- Boss A. P., 2000, *ApJ*, 536, L101
- Bryden G., Chen X., Lin D. N. C., Nelson R. P., Papaloizou J. C. B., 1999, *ApJ*, 514, 344
- Cameron A. G. W., 1978, *Moon & Planets*, 18, 5
- Frank J., Rees M. J., 1976, *MNRAS*, 176, 633
- Kley W., 1999, *MNRAS*, 303, 696
- Laughlin G., Bodenheimer P., 1994, *ApJ*, 436, 335
- Lin D. N. C., Ida S., 1997, *ApJ*, 477, 781
- Lin D. N. C., Papaloizou J. C. B., 1993, in Levy E. H., Lunine J. I., eds, *Protostars and Planets III*. Univ. Arizona Press, Tucson AZ, p. 749
- Lucas P. W., Roche P. F., 2000, *MNRAS*, 314, 858

- Lubow S. H., Siebert M., Artymowicz P., 1999, *ApJ*, 526, 1001
 Marcy G. W., Butler R. P., 1998, *ARA&A*, 36
 Marcy G. W., Butler R. P., 2000, *PASP*, 112, 137
 Marcy G. W. et al., *ApJ*, 2001, in press
 Masunaga H., Inutsuka S. I., 1999, *ApJ*, 510, 822
 Mayor M., Queloz D., 1995, *Nat*, 378, 355
 Motte F., André P., 2001, *A&A*, 365, 440
 Nelson R. P., Papaloizou J. C. B., Masset F. S., Kley W., 2000, *MNRAS*, 318, 18
 Papaloizou J. C. B., Savonije G., 1991, *MNRAS*, 248, 353
 Papaloizou J. C. B., Terquem C., 1999, *ApJ*, 521, 823
 Pickett B. K., Durisen R. H., Cassen P., Mejia A. C., 2000, *ApJ*, 540, L95
 Press W. H., Teukolsky S. A., 1977, *ApJ*, 213, 183
 Press W. H., Teukolsky S. A., Vetterling W. T., Flannery B. P., 1993, *Numerical Recipes in FORTRAN – the Art of Scientific Computing*. Cambridge Univ. Press, Cambridge
 Pudritz R. E., Wilson C. D., Carlstrom J. E., Lay O. P., Hills R. E., Ward-Thompson D., 1996, *ApJ*, 470, L123
 Queloz D., Eggenberger A., Mayor M., Perrier C., Beuzit J. L., Naef D., Sivan J. P., Udry S., 2000, *A&A*, 359, L13
 Quinlan G. D., Tremaine S. D., 1992, *MNRAS*, 259, 505
 Rasio F. A., Ford E. B., 1996, *Sci*, 274, 954
 Stepinski T. F., Black D. C., 2000, *A&A*, 356, 903
 Trilling D. E., Benz W., Guillot T., Lunine J. I., Hubbard W. B., Burrows A., 1998, *ApJ*, 500, 428
 Weidenschilling S. J., Mazari F., 1996, *Nat*, 384, 619
 Zapatero Osorio M. R., Bejar V. J. S., Martin E. L., Rebolo R., Barrado Y., Navascues D., Bailer-Jones C. A. L., Mundt R., 2000, *Sci*, 290, 103

This paper has been typeset from a \TeX/L\AA\TeX file prepared by the author.